Design of a lidar receiver with fiber-optic output

James R. Jenness, Jr., Daniel B. Lysak, Jr., and C. Russell Philbrick

Design considerations for a coaxial lidar receiver are examined, including details of coupling to an optical fiber for transfer of return light to a remote detector box. Attention is concentrated on the influence of fiber position on return-light capture efficiency and dynamic range of the return signal. The effect of a central obstruction on short-range signals is included. The analysis is augmented with simulations of lidar receiver performance. © 1997 Optical Society of America

Key words: Lidar, optical instruments, simulation, remote sensing, atmospheric optics.

1. Introduction

Astronomical telescopes have been modified to serve as lidar receivers with good results.[1] However, the functions differ. A telescope forms diffraction-limited images of distant light sources. A lidar receiver collects return light scattered from a finite laser-illuminated spot at a finite distance. Because a lidar is not an imaging system, the receiver has no eyepiece or photographic plate holder, and no need for a secondary mirror. However, a diagonal mirror is required to transmit the laser beam along the receiver axis. It obstructs a central zone of the collecting mirror.

An optical fiber is convenient for transfer of return light to a remote detector box.[2] It also serves as a field stop to limit the transfer of background light to the detector box. For efficient capture of the convergent ray cone, the fiber's numerical aperture should be compatible with the receiver's f/D ratio.

In general the image of a laser-illuminated spot will not be in sharp focus over the full range covered by a lidar system. Typically, with the fiber at the infinity focus, there is a long-range interval for which the blur disk is small enough for complete capture. There is a transitional range for which the blur-disk diameter is equal to the fiber diameter. For shorter ranges the blur disk is larger, and light falls outside the fiber. For the shortest ranges, obstruction by the diagonal transmitter mirror reduces the signal further.

Background light falls on the full fiber cross section. For the longest ranges, with a sharply focused image smaller than the fiber cross section, the signal–background ratio can be improved by reducing the fiber cross section. However, a smaller fiber drastically reduces the signal from the shortest ranges because of the effect of the central obstruction.

Figure 1 shows an example of a vertical meteorological lidar system. A simple Newtonian receiver has a collecting mirror of diameter D. A central zone of diameter D_t is blocked by the diagonal transmitter mirror. Peripheral rays arrive at the focus at an off-axis angle Ψ determined by

$$\tan \Psi = D/(2f), \tag{1}$$

where f is the focal length of the collecting mirror. The collected light is captured by an optical fiber; the field of view is determined by its cross section.

The requirements for a lidar receiver are to

(1) collect light backscattered from a minimum distance to infinity, and
(2) concentrate the collected light inside a field-stop aperture or optical fiber.

For a typical meteorological lidar system, the Airy disk is small compared to the geometric image of a spot illuminated by the transmitter beam. If the received light is to go into a fiber, the choice of field-stop aperture diameter is limited to available fiber diameters. The numerical aperture of the fiber imposes a lower limit on the ratio f/D.

In this analysis, attention is directed to the transmitter beam, the illuminated spot that moves out with the speed of light after each laser pulse, and the

The authors are with the Applied Research Laboratory, Pennsylvania State University, P.O. Box 30, State College, Pennsylvania 16804.

Received 29 July 1996; revised manuscript received 2 December 1996.
0003-6935/97/184278-07$10.00/0

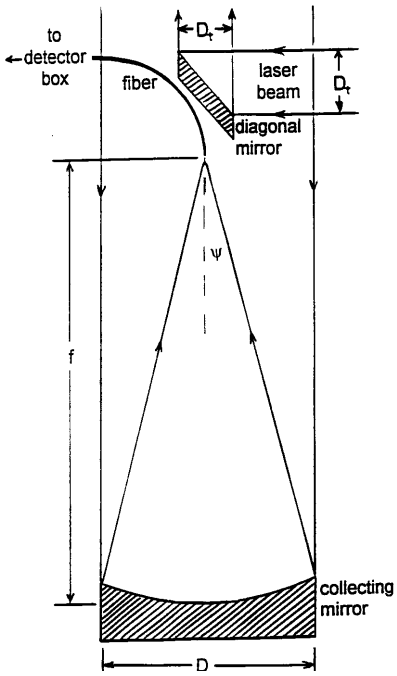

Fig. 1. Lidar optics.

image of the spot. Factors influencing the mating of the receiver with an optical fiber are considered, including out-of-focus effects and blockage of light by the central obstruction. Design constraints are derived, and some design options are examined with the Applied Research Laboratory/Pennsylvania State University (ARL/PSU) lidar simulation.

2. Beam Spot and its Image

In the transmitter design, the laser beam diameter and divergence are traded off. A wider beam has reduced divergence and near-field power density, but increasing the beam diameter requires an increase in the diagonal transmitter mirror profile diameter D_t, blocking more of the collecting mirror profile. The beam starts out with a diameter D_t and a divergence angle θ. At a distance z it has a diameter

$$D_z = D_t + \theta z.$$

The spot illuminated at an altitude z by the vertical beam of a meteorological lidar subtends an angle

$$\Phi = D_z/z. \tag{3a}$$

At a distance v from the collecting mirror the image of the spot subtends the same angle:

$$\Phi = d_i/v. \tag{3b}$$

The image diameter is

$$d_i = vD_z/z. \tag{4}$$

The image distance v is related to z by the lens equation

$$1/v + 1/z = 1/f, \tag{5}$$

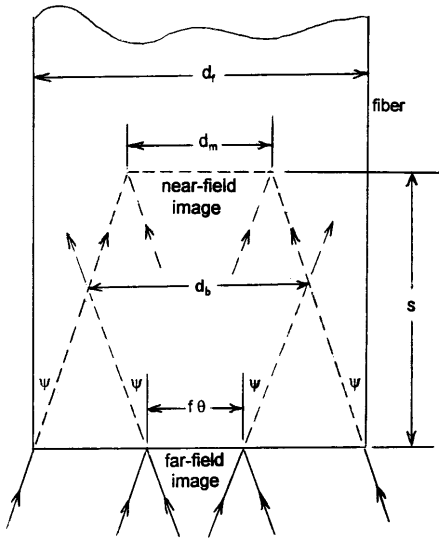

Fig. 2. Capture of images by optical fiber.

from which

$$v = zf/(z - f) \tag{6}$$

Another useful relationship is

$$v - f = f^2/(z - f). \tag{7}$$

For large values of z, Eq. (6) becomes

$$v = f. \tag{8}$$

Combining Eqs. (2), (4), and (6), the image diameter is

$$d_i = (D_t + z\theta)\, f/(z - f). \tag{9}$$

If z is large compared with f, the approximation

$$d_i = f(\theta + D_t/z) \tag{10}$$

is appropriate, and for very large values of z,

$$d_i = f\theta. \tag{11}$$

A fiber of diameter d_f at the infinity focus will capture the image of a far-field spot if $d_f \geq d_i$. This is illustrated in Fig. 2, which shows a side view of a fiber with its end face in the focal plane, capturing a far-field image of diameter $f\theta$. The fiber also captures near-field images within a certain distance beyond the infinity focus, since it intercepts all the rays converging toward them. Because d_f and $f\theta$ are small compared with D, all peripheral rays have off-axis angles very nearly equal to Ψ. Before insertion of the fiber, the intercepted image of maximum diameter is at a distance s beyond the far-field image. From the geometry of Fig. 2 it is evident that the largest near-field image that can be captured by a fiber at the infinity focus has a diameter

$$d_m = d_f - 2s \tan \Psi = d_f - sD/f. \tag{12}$$

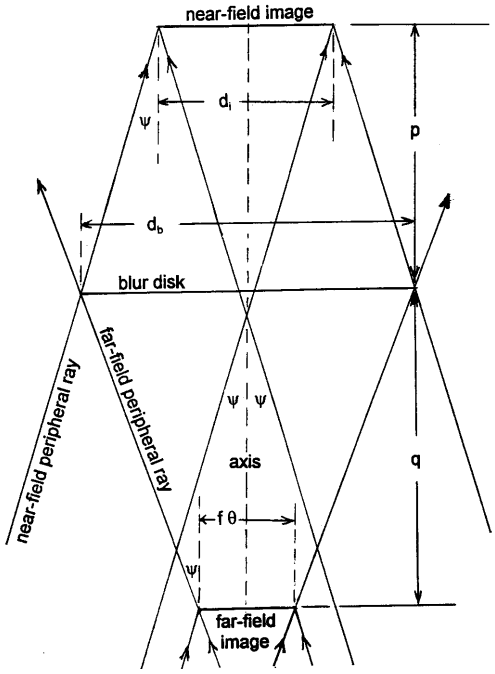

Fig. 3. Peripheral rays converging to edges of near-field and far-field images.

From Eq. (10) this is also

$$d_m = f(\theta + D_t/z_m). \tag{13}$$

This image is at a distance v_m from the collecting mirror. When Eq. (7) is used, with the approximation for z_m large compared with f,

$$s = v_m - f = f^2/z_m. \tag{14}$$

Combining Eqs. (12), (13), and (14) and rearranging, we find that the minimum altitude from which peripheral rays can be captured by a fiber end face at the infinity focus is

$$z_m = f(D + D_t)/(d_f - f\theta).$$

This is a transitional altitude; images of spots above it are captured, and for images of spots below it the capture efficiency is less than 1.

The fiber need not be at the infinity focus. At any position from the focus to s beyond it, the end face will intercept all rays converging toward the near-field image and all rays diverging from the far-field image. The blur disk that includes all these rays has a minimum diameter d_b in an intermediate plane where the peripheral converging and diverging rays intersect.

This is shown in greater detail in Fig. 3. It is evident that

$$d_b = f\theta + 2q \tan \Psi = d_i + 2p \tan \Psi, \tag{16}$$

where q is the distance from the far-field image to the minimum-diameter blur disk and p is the distance from this blur disk to the near-field image.

The distance between the near- and far-field images is

$$p + q = v - f. \tag{17}$$

From Eq. (7),

$$p + q = f^2/(z_t - f), \tag{18}$$

where z_t is the transitional altitude above which all return rays form blur disk with diameters no greater than d_b. If z_t is large compared with f,

$$p + q = f^2/z_t, \tag{19}$$

$$p = f^2/z_t - q. \tag{20}$$

Substituting from Eq. (20) in Eq. (16) and rearranging, we find that

$$q = (1 + D_t/D) f^2/(2z_t), \tag{21}$$

$$p = (1 - D_t/D) f^2/(2z_t). \tag{22}$$

If D_t/D is a small fraction, p and q do not differ greatly, and the minimum-diameter blur disk lies approximately halfway between the near- and far-field images.

Returning to Eq. (16), with substitutions from Eqs. (1) and (21) or (22),

$$d_b = f\theta + (D + D_t) f/(2z_t). \tag{23}$$

An optical fiber end face in the plane of this blur disk will capture all the light in the near- and far-field images (and all intermediate images) if its diameter d_f is greater than d_b. Increasing q increases d_b; there is a maximum-capture position where $d_b = d_f$. Substituting d_f for d_b in Eq. (23) and rearranging, we find that

$$f(D + D_t) = 2z_t(d_f - f\theta). \tag{24}$$

This incorporates the design trade-offs for a lidar system capable of capturing defocused images of beam-illuminated spots at altitude z_t and higher. If D is significantly larger than D_t and d_f is significantly larger than $f\theta$, the trade-off is approximated by

$$fD = 2z_t d_f. \tag{25}$$

The numerical aperture A_n of the fiber sets another constraint. For compatibility with the collecting mirror,

$$A_n = \sin \Psi \tag{26}$$

or

$$f/D = 0.5[(1/A_n)^2 - 1]^{1/2}. \tag{27}$$

With the ratio f/D specified by Eq. (27) and the product fD specified by Eq. (25), the receiver design can be determined.

From Eq. (24), the transitional altitude for a system with the fiber in the maximum-capture position at the distance q behind the infinity focus is

$$z_t = (D + D_t)/[2(d_f/f - \theta)]. \tag{28}$$

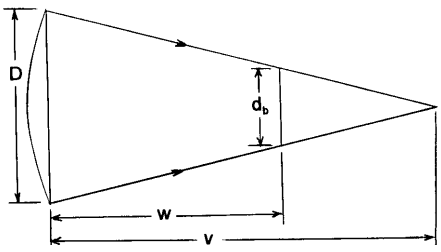

Fig. 4. Equivalent lens.

This is less than the corresponding altitude z_m for a system with the fiber at the infinity focus. It is the lowest altitude for which the beam-spot image is completely captured by a fiber of diameter d_f. With a fiber of numerical aperture 0.2, Eq. (27) specifies $f = \sqrt{6}\,D$ and

$$z_t = (D + D_t)/[2(d_f/\sqrt{6}D - \theta)]. \tag{29}$$

This is the lowest altitude for which all the return collected by a mirror of diameter D from a spot illuminated by a beam with divergence θ and initial diameter D_t can be captured by a fiber of diameter d_f and numerical aperture 0.2.

For altitudes below z_t, the blur disk is larger, some of the light falls outside the fiber, and the capture efficiency decreases with decreasing altitude. For a first-order estimate of light capture from spots below the transition altitude z_t, consider the case of an equivalent lens, Fig. 4, with rays converging to a near-field focus at a distance v. At a distance w the blur disk diameter is

$$d_b = (v - w)D/v. \tag{30}$$

When we substitute for v from Eq. (6), the result is

$$d_b = [z(f - w) + wf]D/(zf). \tag{32}$$

The infinity focus is not the fiber position for maximum light capture, but the maximum-capture position is near the focus. With the approximation $w = f$,

$$d_b = fD/z. \tag{32}$$

With a blur disk larger than the fiber cross section, the light-capture efficiency is

$$(d_f/d_b)^2 = d_f^2 z^2/(fD)^2. \tag{33}$$

This indicates an increasing capture efficiency with increasing z until d_b decreases to d_f at the transitional altitude, Eq. (28). For higher altitudes the efficiency is 1; all return light falling on the collecting mirror is captured. As the altitude increases, the blur disk shrinks inside the fiber cross section, and the signal–background ratio decreases.

The intensity of the return light varies as $1/z^2$, and at altitudes below z_t this cancels the factor z^2 in Eq. (33). This predicts a signal strength that does not vary with z at lower altitudes, as shown in a standard lidar text[3] and demonstrated by a simulation.[4] It neglects the obstruction of the diagonal transmitter mirror. A subsequent analysis[5] considers the effect of the central obstruction on returns from altitudes above 100 m. It is of interest to include lower altitudes.

3. Central Obstruction

The profile of the diagonal mirror sets a low-altitude limit for light capture by the fiber. For a near-field ray trace, Fig. 5 represents the system of Fig. 1 as an equivalent lens of diameter D with a central obstruction of diameter D_o.

Light from the center of a beam spot at altitude z_o comes to a focus at a distance v_o behind the lens. By Eq. (6),

$$v_o = z_o f/(z_o - f). \tag{34}$$

Rays converging toward this dark focus pass outside the fiber face; the central obstruction blocks rays inside the cone subtended by the fiber face of diameter d_f. By the geometry of Fig. 4,

$$v_o/D_o = [v_o - (f + q)]/d_f. \tag{35}$$

Substituting for v_o from Eq. (34) and rearranging, we find that the corresponding altitude is

$$z_o = f/[1 - f(1 - d_f/D_o)/(f + q)]. \tag{36}$$

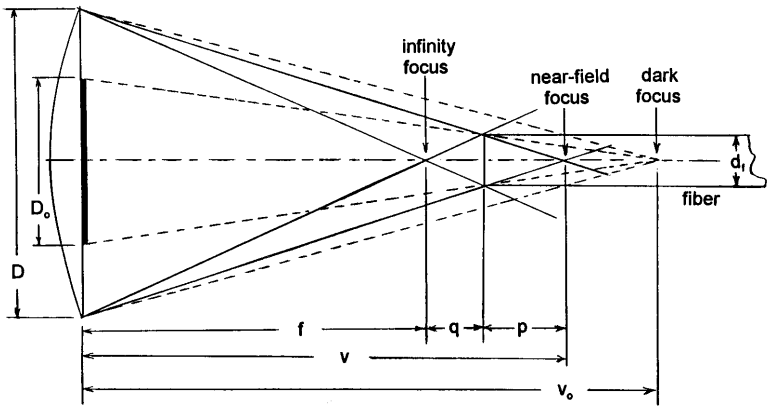

Fig. 5. Lens system equivalent to lidar receiver with central obstruction.

Because q is small compared with f, this is approximately

$$z_o = fD_o/d_f. \quad (37)$$

Light from the center of a beam spot at this altitude is not captured, but the fiber still receives light from off-axis points. A larger portion of the light from beam spots at lower altitudes is blocked. We can reduce the blockage by reducing D_o, but it can be no less than D_t.

In some lidar systems it may be possible to eliminate the central obstruction by use of a beam splitter or polarizer to transmit the laser beam without obscuring the return light.

4. Design Envelope

For maximum light collection, D has the largest value compatible with cost and mechanical constraints. For capture of the collected light by an optical fiber, the optimum value of f is determined by D and the fiber's numerical aperture, Eq. (27).

The diameter of the spot illuminated at altitude z is given by Eq. (2). All the light in the image of a spot above a minimum altitude z_m, Eq. (15), is captured by a fiber of diameter d_f at the infinity focus. A fiber at a distance q behind the focus will have a capture efficiency of 1 for returns from a lower transitional altitude z_t, Eq. (28). A limiting altitude z_o, below which the central obstruction begins to block return light, is given by Eq. (36). These altitudes and the optimum focal length are compiled in Table 1 as functions of D for a system with a fiber of 1-mm diameter and numerical aperture 0.2, with $D_o = D_t = 5$ cm and $\theta = 0.09$ mrad.

The receiver for the ARL/PSU lidar atmospheric measurements profiler (LAMP)[1] is a Cassegrain telescope whose secondary mirror blocks a central area of diameter $D_o = 13.2$ cm, much larger than the profile diameter of the diagonal transmitter mirror. With $D = 40.64$ cm (16 in.) and an effective focal length of 603 cm, its transition altitude is much greater than that for $D = 40$ cm in Table 1, which is based on a focal length of 98 cm, with the smaller central obstruction diameter $D_o = D_t = 5$ cm.

A next-generation Newtonian receiver with 1/6 the LAMP focal length will show improved low-altitude performance. It is of interest to simulate a system with $D = 40$ cm, $D_t = 5$ cm, and $f = 100$ cm. Equation (33), based on the uniformly illuminated blur-disk model,[3,4] is not accurate for computation of capture efficiencies less than 1. The model must include the laser beam's Gaussian profile as well as the central obstruction.

5. Gaussian Beam

Equation (2) gives the cross-sectional diameter of a conical beam produced by a point source at a distance D_t/θ behind an aperture of diameter D_t. The cross section of such a beam is illuminated uniformly. This simple model is adequate for estimating z_o, z_t, and z_m, but not for computing the capture efficiency.

Table 1. Critical Altitudes for Light Capture by an Optical Fiber of 1-mm Diameter as Functions of Collecting Mirror Diameter[a]

D (cm)	f (cm)	z_o (m)	z_t (m)	z_m (m)
10	24.5	8.2	18.5	37.8
20	49.0	19.8	63.6	128.6
30	73.5	31.8	137.0	276.1
40	98.0	44.0	240.8	484.5
50	122.5	56.3	377.3	758.3
60	147.0	68.9	549.0	1102.4
70	171.5	80.9	758.6	1522.4
80	196.0	93.3	1009.2	2024.3
90	220.5	105.6	1304.1	2614.9
100	244.9	118.0	1647.2	3301.8

[a]Diagonal mirror profiel diameter: 5 cm. Beam divergence: 0.09 mrad. Focal length is 2.45 D to match fiber numerical aperture of 0.2.

Instead of the uniform illuminator, the beam model in the ARL/PSU lidar simulation has a Gaussian radial profile.

The simulation transmits Gaussian-weighted rays to 200 points distributed over the beam cross section. From each of these points they are scattered to 10^5 points on the collecting mirror; $2(10^7)$ rays are traced. Return rays blocked by the central obstruction are deleted. The simulation computes the portion of the light incident on the collecting mirror that subsequently arrives inside a fiber. This is the capture efficiency. The intensity of the light in the blur disc varies as the inverse square of the distance to the beam spot, so a z^2 factor produces a quantity proportional to the total captured light power. This is an index of the return signal strength. With the effect of the central obstruction included, the simulation gives an estimate of the relative signal strength down to altitudes just above the telescope.

A few preliminary calculations are required to set up a simulation of a system with 1/6 the LAMP focal length. Table 1 shows a transitional altitude of 240.8 m for a system with $D = 40$ cm and $f = 98$ cm. With these values of z_t and f, the fiber position for maximum light capture is $q = 2.24$ mm beyond the focal plane. Figure 6 shows the computed capture efficiency and the relative signal strength, the product of the capture efficiency, and the z^2 factor. The capture efficiency increases to 1.0 at 240.8 m, the z_t value for $D = 40$ cm in Table 1. The signal strength is 1.0 at 1000 m, taken as the reference distance for the z^2 factor. The capture efficiency falls below 0.01 at 50 m, but the z^2 factor boosts the simulated output signal strength to approximately 3.5.

The inverse-square increase in intensity compensates for the reduced capture efficiency at lower altitudes. When we place the fiber at the maximum-capture position, the capture efficiency is increased at lower altitudes where it is not needed, which increases the dynamic range of the signal. Figure 7 compares the signals in fibers at the infinity focus and the maximum-capture position 2.24 mm beyond it. With the fiber at the infinity focus, the signal is

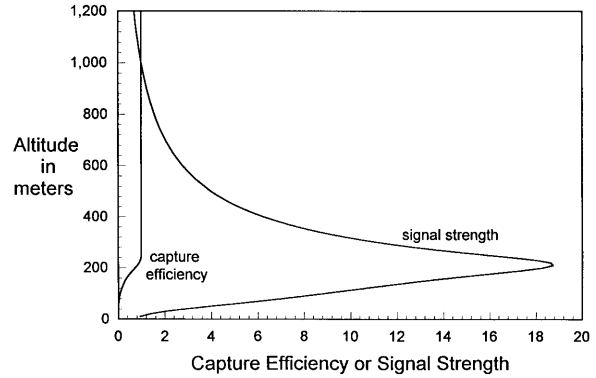

Fig. 6. Capture efficiency and signal strength for a 1-mm fiber at the maximum-capture position of a mirror of 40-cm diameter and 100-cm focal length.

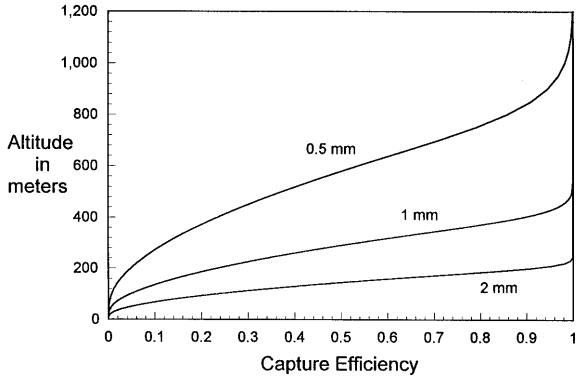

Fig. 8. Capture efficiencies for 0.5-, 1.0-, and 2.0-mm fibers at the infinity focus of a mirror of 40-cm diameter and 100-cm focal length.

the same for altitudes above 450 m and lower for lower altitudes, reducing the dynamic range. The lowest altitude at which a usable signal can be obtained is reduced only slightly by moving from the infinity focus to the maximum-capture position.

It is also of interest to consider the effect of fiber diameter, Fig. 8. For an altitude of 500 m or lower, a 2-mm fiber at the infinity focus has a greater capture efficiency than a 1-mm fiber. It also has a greater capture efficiency than a 1-mm fiber at its maximum-capture position (Fig. 6).

Figure 9 shows the results of applying the z^2 factor to the capture efficiencies in Fig. 8. The main result of increased fiber diameter is an increase in the dynamic range of the signal. On the other hand, all the fibers have an equal signal strength for altitudes above 1000 m. For low altitudes, the blur disk is larger than the fiber cross section. The 1.0- and 0.5-mm fibers capture light over a relatively small central area, within which the variation of the blur-disk light intensity is limited. The result is similar to that for the uniformly illuminated blur-disk model,[3,4] the curves for the smaller fibers have quasi-flattops over a finite altitude interval. The central obstruction decreases the signal at the lowest altitudes.

6. Discussion

A lidar receiver optimized for fiber-optic output has a smaller f/D ratio than a typical astronomical telescope. Of course the quantity f/D does not have the same significance for a nonimaging system. The distribution of light in the focal plane is not important if a blurred high-altitude beam-spot image can be captured, and a significant fraction of the light in low-altitude images can also be captured.

Larger fibers capture more low-altitude light, but they admit more background light than smaller fibers, reducing the high-altitude signal–background ratio. To minimize sky background at a given altitude, the field of view d_f/f should be equal to the angle Φ subtended by the beam spot. At the highest altitudes, Φ approaches the beam divergence angle θ. Background reduction is traded off against capture efficiency over the altitude interval of interest.

Light capture is maximized with the fiber at the distance q behind the infinity focus. However, the capture enhancement is concentrated at lower altitudes. This configuration or a larger fiber has merit for altitudes below 1 km. For high-altitude systems, fiber placement at the infinity focus reduces the dynamic range of the output. A high-altitude system

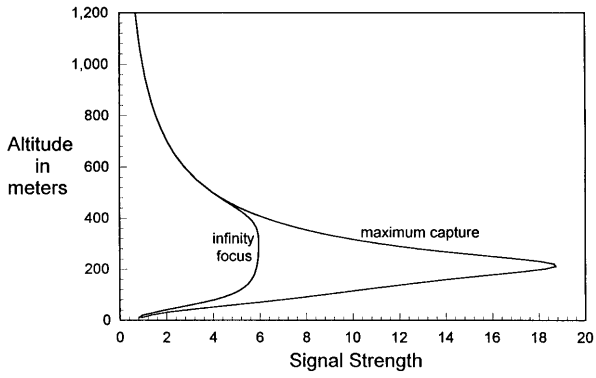

Fig. 7. Signal strength for a 1-mm fiber at the maximum-capture position and the infinity focus of a mirror of 40-cm diameter and 100-cm focal length.

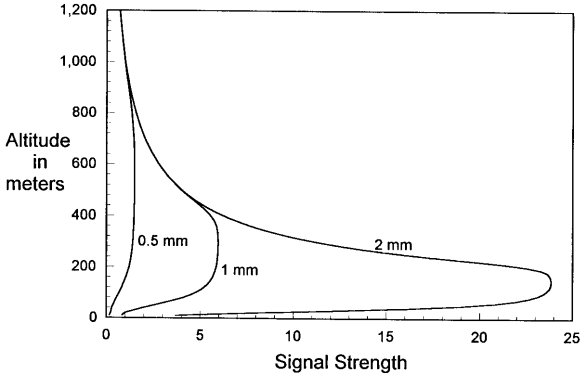

Fig. 9. Signal strength for 0.5-, 1.0-, and 2.0-mm fibers at the infinity focus of a mirror of 40-cm diameter and 100-cm focal length.

can achieve adequate light capture and increased signal–background ratio with a smaller fiber.

For a given fiber diameter, the minimum altitude for complete capture is achieved with f and D at the limits defined by Eqs. (25) and (27). This indicates that a collecting mirror of 40-cm diameter should have a focal length of approximately 100 cm to maximize light capture by a 1-mm fiber with 0.2 numerical aperture. Table 1 shows a transitional altitude of 240.8 m for such a system. This is the altitude at which the capture efficiency increases to 1 in Fig. 6.

The inverse-square effect reduces the high-altitude signal, and the central obstruction effect reduces the low-altitude signal. If the emphasis is on low-altitude performance, adequate signal strength may be achieved with a lower-powered laser and less beam expansion (smaller D_o) to reduce the altitude z_o.

A focal-reducer lens[6] reduces the blur-disk diameter and increases the numerical aperture. This can match a telescope with large f/D to a fiber's numerical aperture. However, adding on another component increases the number of misalignment degrees of freedom. Also, in a multiwavelength system there can be a significant axial separation between the foci of a lens for the different wavelengths. A simple Newtonian system (Fig. 1) with the collecting mirror's f/D matched to the fiber's numerical aperture will have reduced overall length, leading to a compact mechanical design.

To capture a significant fraction of the light in a defocused low-altitude image, a fiber must have a diameter much larger than the Airy disk. Such a fiber can capture all the light in the image of a high-altitude spot. The collecting mirror need not be diffraction-limited. The performance of such a mirror can be specified in terms of light concentration inside an aperture with approximately 1/10 the diameter of the fiber. Such a test has been applied[7,8] to paraboloidal mirrors with f/D as small as 0.9. Centrifugal forming of mercury in a rotating container[7,9,10] is an interesting technique for generating a paraboloidal surface of reduced f/D for a system with a vertical optic axis.

7. Conclusions

The diameter of a beam-spot image is proportional to a lidar receiver's focal length. A small image, and therefore a short focal length, is desirable to facilitate capture by an optical fiber.

A mirror of large diameter is desirable for increased light collection. If light collected by a mirror of a given diameter D is to be captured by a fiber, the minimum of the ratio f/D, and therefore the minimum focal length f, is determined by the numerical aperture of the fiber.

The fiber position for maximum light capture is beyond the infinity focus. However, maximum capture is not usually required. The inverse-square increase in the intensity of the return light compensates for the decrease in capture efficiency over a finite altitude interval. A fiber at the infinity focus will achieve adequate light capture over a large altitude interval, with less dynamic range in the output signal.

A meteorological lidar receiver is not an imaging system; it is a light-collecting system. Diffraction-limited optics are not required. Adequate performance is achieved if the high-altitude image is smaller than the fiber end face. If adequate light is captured from the highest altitude of interest, the return from lower altitudes will be much greater.

The low-altitude signal strength is reduced by the central obstruction of a coaxial transmitter mirror. Reducing the diameter of the obstruction enhances low-altitude performance. This is traded off against expansion of the laser beam to reduce its intensity and divergence.

This research was sponsored by the Oceanographer of the Navy through the U.S. Navy Environmental Systems Program of the Space and Naval Warfare Systems Command.

References

1. C. R. Philbrick, D. B. Lysak, T. D. Stevens, P. A. T. Haris, and Y. C. Rau, "Atmospheric measurements using the LAMP lidar during the LADIMAS campaign," in *Sixteenth International Laser Radar Conference*, NASA Conf. Publ. 3158, Part 2. (NASA, Hampton, Va., 1992), pp. 651–654.
2. P. Keckhut, A. Hauchecorne, and M. L. Chanin, "Critical review of the data base acquired for the long-term surveillance of the middle atmosphere by the French lidars," J. Atmos. Oceanic. Technol. **10,** 850–861 (1993).
3. R. M. Measures, *Laser Remote Sensing* (Krieger, Malabar, Fla. 1992), p. 260.
4. J. Harms, W. Lahmann, and C. Weitkamp, "Geometrical compression of lidar return signals," Appl. Opt. **17,** 1131–1135 (1978).
5. J. Harms, "Lidar return signals for coaxial and noncoaxial systems with central obstruction," Appl. Opt. **18,** 1559–1566 (1979).
6. H. Rutten and M. Venrooij, *Telescope Optics* (Willman-Bell, Richmond, Va., 1988), p. 153.
7. G. Hass and J. R. Jenness, Jr., "Method for fabricating paraboloidal mirrors," J. Opt. Soc. Am. A. **48,** 86–87 (1958).
8. J. H. Saxton and D. E. Kline, "Optical characteristics and physical properties of filled-epoxy mirrors," J. Opt. Soc. Am. A. **50,** 1103–1111 (1960).
9. R. W. Wood, "The mercury paraboloid as a reflecting telescope," Astrophys. J. **29,** 164–176 (1909).
10. R. J. Sica, S. Sargoytchev, S. Flatt, E. Borra, and L. Girard, "Lidar measurements using large liquid mirror telescopes," in *Sixteenth International Laser Radar Conference*, NASA Conf. Pub. 3158, Part 2. (NASA, Hampton, Va., 1992), pp. 655–658.